Supporting Information

Achieving high performance poly(vinylidene fluoride) dielectric composites via *in-situ* polymerization of polypyrrole nanoparticles on hydroxylated-$BaTiO_3$ particles

Xu Xie,[1] Zhen-zhen He,[1] Xiao-dong Qi,[1] Jing-hui Yang,[1] Yan-zhou Lei,[2] Yong Wang*[1]

1. School of Materials Science & Engineering, Key Laboratory of Advanced Technologies of Materials (Ministry of Education), Southwest Jiaotong University, Chengdu, 610031, China
2. Analytical and Testing Center, Southwest Jiaotong University, Chengdu, 610031, China

- **Experimental Part**

Microstructure characterizations

A thermal gravimetric analysis (TGA) TG 209 F3 Tarsus (Netzsch, Germany) was used to detect the hydroxylation degree of BT. During the measurements, sample of about 8 mg was initially preserved at 100 °C for 3 min to eliminate the moisture. Then, the sample was quickly cooled down to 30 ℃. After that, the sample was heated to 800 ℃ at a heating rate of 10 ℃/min. The measurements were carried out in nitrogen atmosphere.

A differential scanning calorimeter (DSC) STA449C Jupiter (Netzsch, Germany) was used to investigate the melting and crystallization behaviors of the composite samples. During the measurement, sample of about 8 mg was heated from 30 °C to 200 °C at a heating rate of 10 °C/min and maintained at 200 °C for 3 min to erase thermal history, then the sample was cooled down to 30 °C at a cooling rate of 5 °C/min. The measurements were carried out in nitrogen atmosphere.

Thermal conductivity measurements

The thermal conductivity of sample was measured on a Transient Hot Disk TPS 2500S instrument (Hot Disk AB, Gothenburg, Sweden) according to the international measuring standard ISO/CD 22007-2.

* Corresponding author: Tel: +86 28 87603042;
E-mail: yongwang1976@163.com

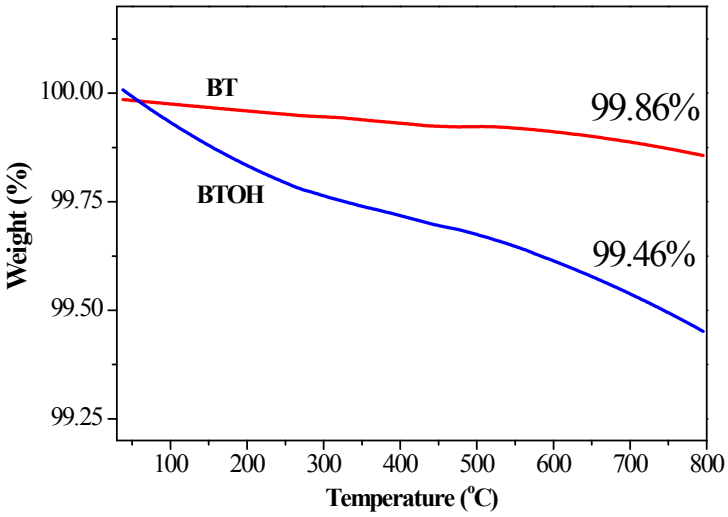

Figure S1. TGA curves of the BT and BTOH nanoparticles as prepared.

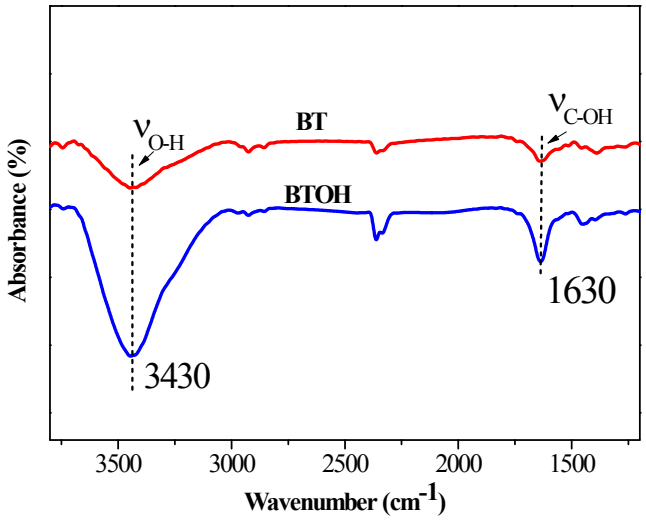

Figure S2. FTIR spectra of BT and BTOH particles as obtained.

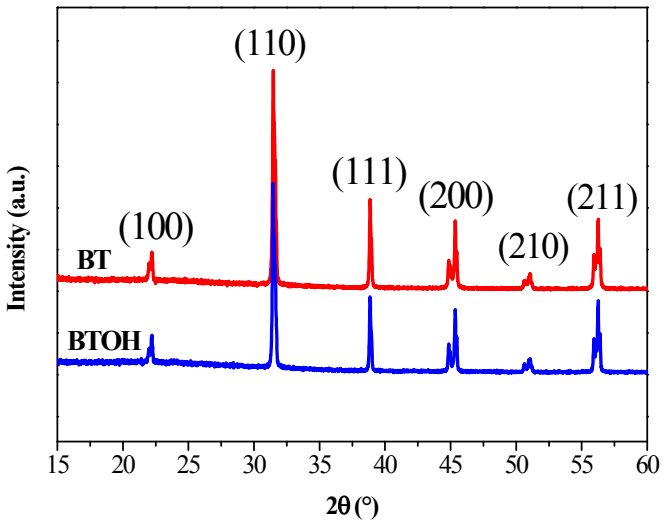

Figure S3. WAXD profiles of the BT and BTOH particles as obtained.

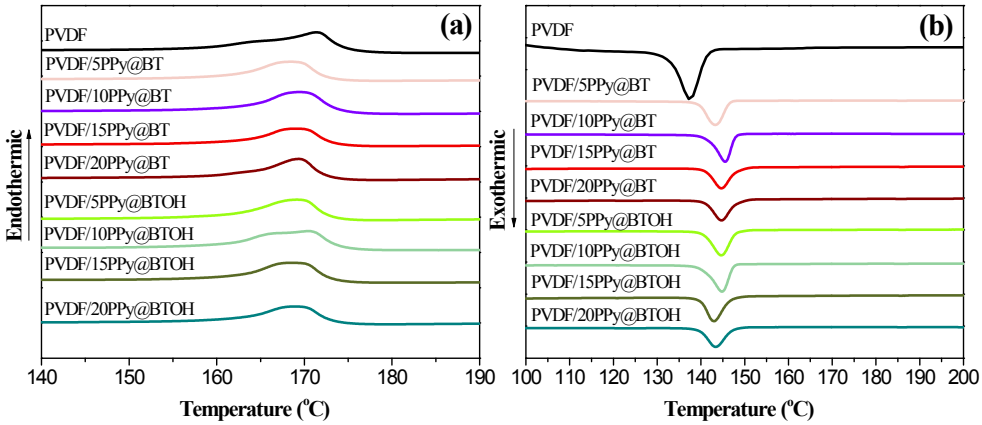

Figure S4. DSC heating curves (a) and cooling curves (b) showing the melting and crystallization behaviors of the PVDF/PPy@BT and PVDF/PPy@BTOH composites.

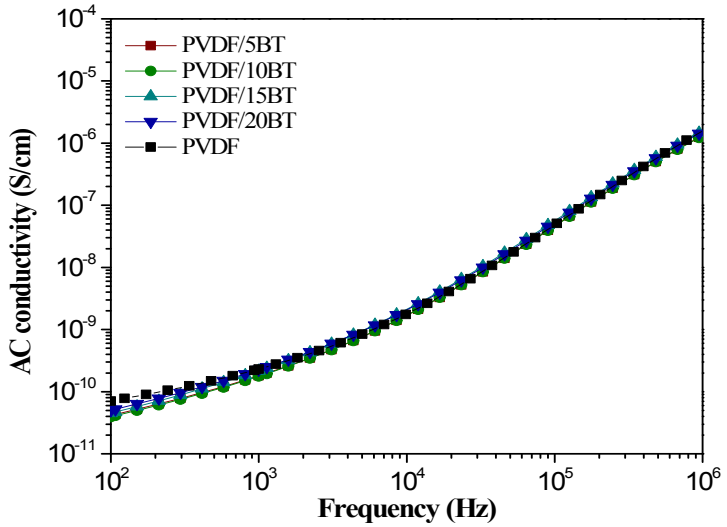

Figure S5. Variation of electrical conductivity of the PVDF/BT composites with increasing BT content.

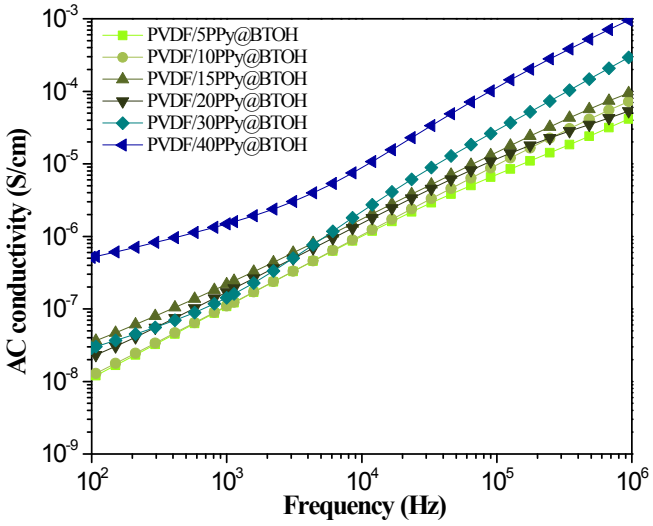

Figure S6. Variation of the AC conductivity of the PVDF/PPy@BTOH composites with increasing content of PPy@BTOH composite particles.

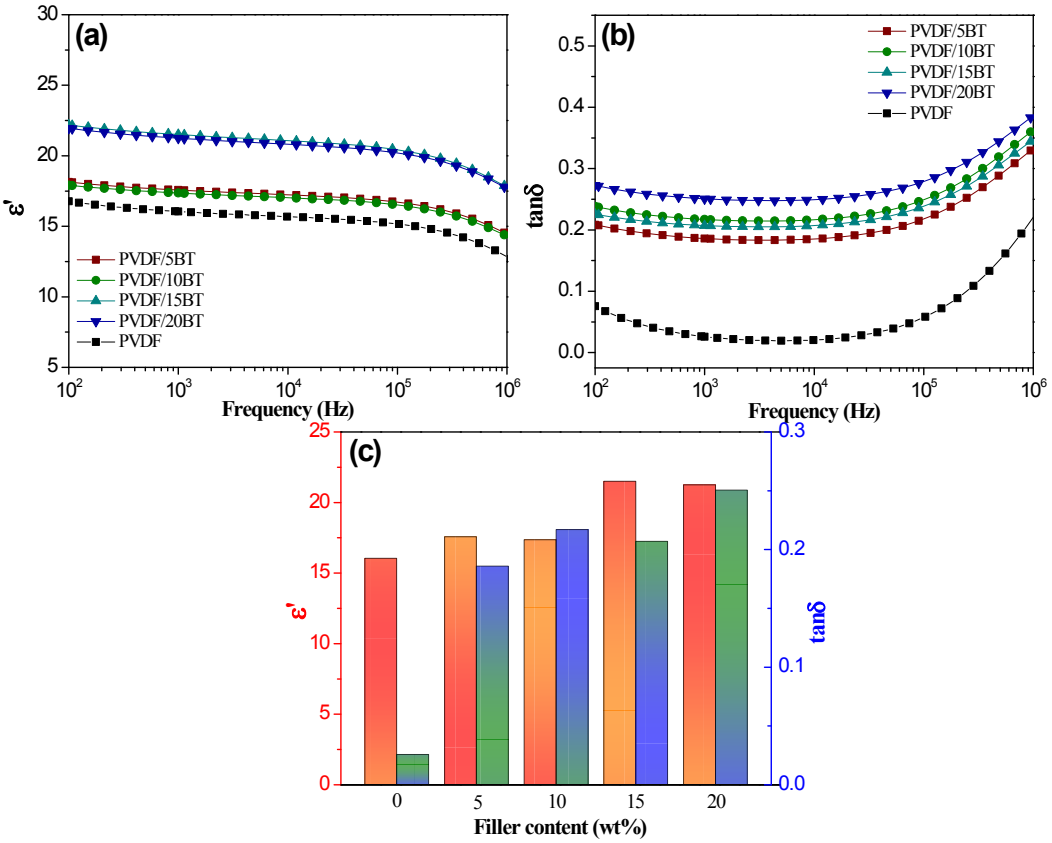

Figure S7. (a) Dielectric constant and (b) dielectric loss of the pure PVDF and PVDF/BT composites, and (c) showing the comparison of dielectric constant and dielectric loss of samples obtained at 1000 Hz.

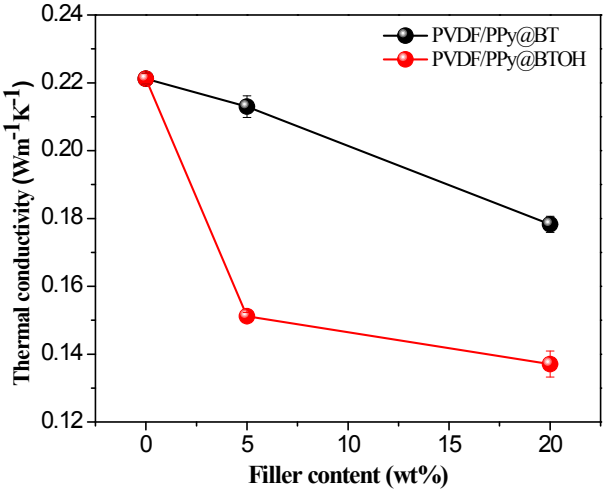

Figure S8. Comparison of the thermal conductivities between the PVDF/PPy@BT and

PVDF/PPy@BTOH composites.